Solution characterization of zirconium oxo clusters

Dietger Van den Eynden,[†] Ajmal Roshan Unniram Parambil,[†] Sandor Balog,[‡] and Jonathan De Roo[*,†]

[†]*Department of Chemistry, University of Basel, Mattenstrasse 24a, 4058 Basel, Switzerland*

[‡]*Adolphe Merkle Institute, University of Fribourg, 1700 Fribourg, Switzerland*

E-mail: jonathan.deroo@unibas.ch

Abstract

Group 4 metal oxo clusters are atomically precise models for colloidal nanocrystals as they consist of an inorganic core and an organic ligand shell. They are also important building blocks for MOFs, 3D-printing and polymers composites. Recently, we have elucidated their structure and ligand shell using solid state methods. Here we go one step further studying these materials in solution. Dynamic light scattering is a common technique to determine the solvodynamic diameter of nanocrystals. However, due to their small size, clusters present difficulties to the automatic data treatment, available in commercial software. Here we developed a data treatment method to fit DLS data of clusters, where we separate the signal into a contribution from the clusters itself combined with a contribution of number fluctuations. Additionally, diffusion ordered spectroscopy (DOSY) is used to study how these materials affect the viscosity of the solvent.

Introduction

Group 4 metal oxo clusters are very interesting materials for material science as they can be used as building blocks in MOFs[1] and 3D-printing.[2] Additionally, due to their small size they show great potential in catalysis.[3] Historically, single crystal XRD was the main characterization technique in order to obtain structural data, requiring the synthesis to be carried out with short and rigid ligands.[4] Zirconium and hafnium clusters form octahedron shaped structures, $M_6O_4(OH)_4(RCOO)_{12}$,with on each corner a metal atom and on each triangular face an O-atom or OH-group.[5] The 12+ positively charged inorganic cores are charge stabilized with 12 organic carboxylate ligands ($RCOO^-$) surrounding the core, thus creating a hybrid object (**Figure 1**). These clusters exist as monomers, $M_6O_4(OH)_4(RCOO)_{12}$ (from here on referred to as **Zr6**), or dimers, $[M_6O_4(OH)_4(RCOO)_{12}]_2$ (from here on referred to as **Zr12**). In the latter, four ligands are connecting 2 octahedra through a bridging binding mode. We found that this dimerization depends solely on the sterical hindrance on the alpha position of the carboxylic acid. For carboxylates with an R group on the alpha position (e.g., methylbutanoic acid) the monomer (**Zr6**) is formed. If the carbon on the alpha position is a CH_2, the clusters dimerize into a **Zr12** regardless of the length of the ligands. These oxo cluster can be seen as the smallest possible oxide nanoparticles.

Because of the short and rigid ligands, the solubility was rather limited precluding extensive characterization in solution. NMR has been used most often to study the surface chemistry, e.g. ligand exchange, however it is not straightforward to distinguish monomers from dimers.[6] This limited the possibility of studying these clusters in solution. Questions like: does the dimer persists in solution and does this depend on the solvent, are difficult to answer.

In recent work we use total scattering and Pair Distribution Function analysis to study clusters that are capped with longer carboxylic acids, inspired by the nanocrystal field.[7] While Dynamic Light Scattering (DLS) is another common technique to study nanocrystals, the oxo clusters (0.5 nm) are at the lower detection limit of common DLS devices. Addition-

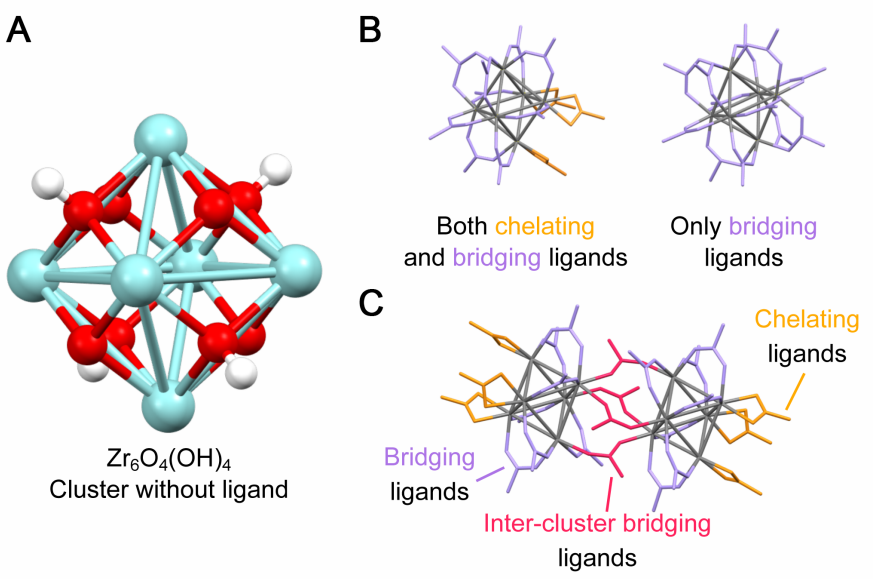

Figure 1: (A) The octahedron shaped cluster core containing six Zr atoms held together by eight O atoms of which four are protonated. (B) The different types of monomeric clusters that have been reported in literature. (C) The dimeric cluster where four ligands are connecting two octahedra.

ally, the data processing is a black box leaving the experimenter blind about data fitting. These challenges inspired us to develop our own data processing method to characterize our cluster samples using DLS.

Here we set out to study the clusters that we previously synthesized and characterized in solution rather than as pure compounds. Therefore, we measured the materials in a common DLS device but fitted the data manually. As it turns out the concentration of our clusters solutions need to be relatively high and they always suffer from number fluctuations, complicating the data processing. We show here how the data can be processed when measuring samples that are nearing the lower detection limits of DLS. Additionally, we studied the behavior of the clusters in solution using Diffusion Ordered Spectroscopy (DOSY) NMR. Since we can estimate the size of the clusters, seeing as they are atomically precise i.e. polydispersity is 0 (in contrast to nanocrystals), we can rearrange the Stokes-Einstein equation and get an estimate of the viscosity of the sample, this way we can study how adding the clusters influences the viscosity of the solvent.

Results

The solvodynamic radius via Dynamic Light Scattering

Zirconium oxo clusters with $M_6O_4(OH)_4$ as a core were synthesized and capped with a range of ligands: propionic (C3), butanoic (C4), hexanoic (C6), octanoic (C8), decanoic (C10), dodecanoic (C12), oleic (C18), methylbutanoic (C5') and methylheptanoic acid (C8'). We optimized the synthesis and purification in previous work.[7] The cluster were dissolved in chloroform and dynamic light scattering measurements were performed in a Malvern Zetasizer Ultra with a 633 nm laser. Taking first **Zr12**-butanoate, different concentrations of cluster were measured to find the optimum. As can be seen in Figure 2A, the lowest concentrations (0.1 and 1 mg/mL), do not show much signal apart from the solvent background. Upon increasing the concentration, irregularities in the intensity plot are observed , indicating that the samples suffer from number fluctuations. Additionally, the samples with these concentrations were measured 20 times and visually the sample with a concentration of 10 mg/mL looks the most consistent (See **Figure S1-S4**).

Therefore, the clusters are measured with a 10 mg/mL concentration in chloroform, in order to have enough signal while limiting the number fluctuations.

Figure 2B shows the intensity auto-correlation functions, which exhibit two main features: an initial fast relaxation, which is well reproducible, and a subsequent series of slow relaxations, whose amplitude and rate showed considerable within-run variations. According to light-scattering phenomena described elsewhere,[8] we attribute the first (fast) relaxation to coherent scattering from clusters undergoing unrestricted Brownian motion. In contrast, the second (slow) relaxation is attributed to the fluctuation in the number of scattering entities in the scattering volume. This phenomenon is referred to as number fluctuations.[9] The scattering volume is defined by the intersection of the laser beam and the field of view of the detection optics and is small, being on the order of nanoliters.[10] Number fluctuations in these experiments do not contain useful information about particle size. Therefore, we

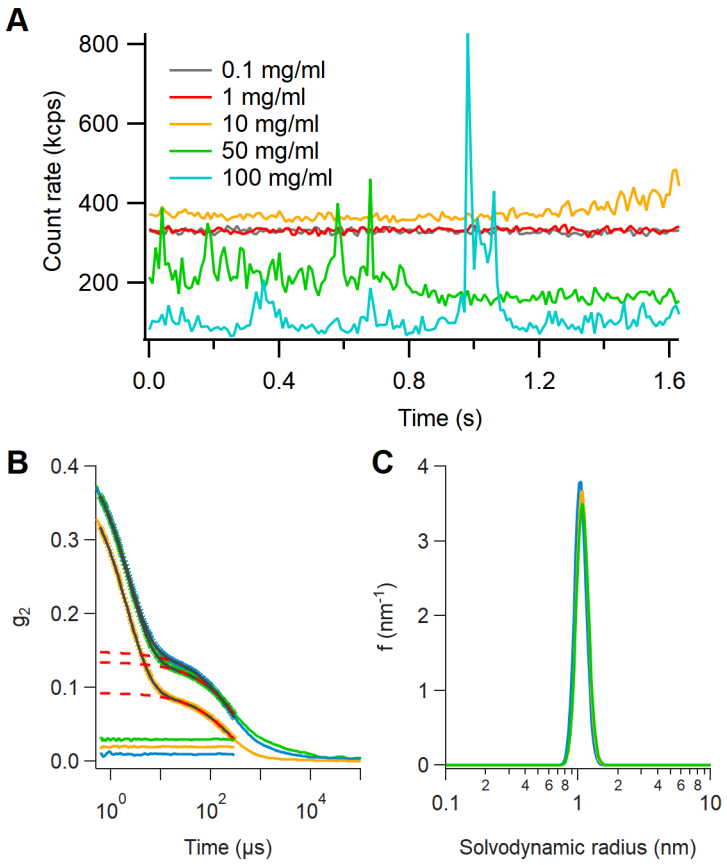

Figure 2: (A) Intensity plot as a function of time for the **Zr12**-butanoate clusters at different concentrations in $CHCl_3$. The lowest concentrations, 0.1 and 1 mg/mL do not show much signal, mainly solvent. Whereas the higher concentrations, 50 and 100 mg/mL show irregular baselines indicating that these samples suffer from number fluctuations. (B) Intensity auto-correlation functions and (C) particle size distribution of **Zr12**-butanoate clusters after manual fitting.

use only the first relaxation for particle sizing via the Stokes-Einstein theory, and the second one is not of any interest.

In the presence of number fluctuations, the intensity-auto-correlation function (also known as the second-order coherence/correlation function) may be modelled by a sum of three terms:[8]

$$g_2(t) - 1 \cong y^2 \mid g_1(t) \mid^2 + 2y(1-y) \mid g_1(t) \mid + (1-y)^2 g_{NF}(t) \tag{1}$$

where $g_1(t)$ is the so-called field auto-correlation function (also known as first-order co-

herence) of the light scattered coherently off the particles undergoing Brownian diffusion, and $g_{NF}(t)$ is the term representing number fluctuations. The positive constants expressed via $1 > y > 0$ are the weights of the linear combination. The first two terms—in our case, appears as the fast relaxation—contain information about particle dynamics, and the last terms appears as the slow relaxation. These two decays have partial overlap, and while their distinction is critical, subsequent separation from one another is not trivial. In the absence of number fluctuations, the relation would be expressed as $g_2(t) - 1 =\mid g_1(t) \mid^2$, which is known as the Siegert relation.[11]

For clusters of identical solvodynamic radius, the field-auto correlation function decays exponentially: $g_1(t) = e^{-\Gamma t}$ with an exponent of $\Gamma = q^2 \frac{k_B T}{6\pi\eta} \frac{1}{r}$ (Stokes-Einstein relation), where r is the solvodynamic (solvodynamic) radius, k_B the Boltzmann constant, T the temperature, (the viscosity of the solvent, $q = \frac{4\pi}{\lambda} n \sin(\frac{\theta}{2})$ is the amplitude of the scattering vector (also known as momentum transfer), θ the scattering angle, λ the wavelength of the scattered light, and n the refractive index of the solution.[12–15]

Polydispersity, in our case a smooth distribution of the solvodynamic radius and thus Γ, affects the relaxation of $g_1(t)$, which may be expressed via an integral equation

$$g_1(t) = \int p(\Gamma) e^{-\Gamma t} d\Gamma \tag{2}$$

An equivalently formula may be given via the solvodynamic radius

$$g_1(t) = \int p(r) e^{-\Gamma(r) t} dr \tag{3}$$

where $p(r)$ is the so-called scattering-intensity-weighted distribution of the solvodynamic radius. These two distribution, $p(r)$ and $p(\Gamma)$, are closely related, one may be obtained from the another by applying the rule of transforming random variables.[16] For example, the probability density function of the intensity-weighted solvodynamic radius is given by

$$p(r) = p(\Gamma(r)) \cdot \left| \frac{d}{dr} \Gamma(r) \right| \tag{4}$$

Our goal is to formulate a parametric model of Equation **1**, to regress the mathematical model against the experimental data. By this, we simultaneously aim to a) separate number fluctuations $g_{NF}(t)$ from coherent scattering, and b) analyze the corresponding fast relaxation $g_1(t)$ in terms of solvodynamic radius distribution.

Given that the clusters are expected to exhibit a modest distribution, we model $g_1(t)$ via a reparametrized form of the Gamma distribution, which is also known as the Schulz–Zimm distribution.[17–19] Accordingly, via the definition of the Gamma distribution and rule of transforming random variables, the distribution of the solvodynamic radius may be expressed via two parameters

$$p(r) = \frac{e^{-\frac{r_Z}{r \cdot \mathrm{PdI}}} \cdot \left(\frac{r_Z}{\mathrm{PdI} \cdot r}\right)^{1/\mathrm{PdI}}}{r \cdot \gamma\left(\frac{1}{\mathrm{PdI}}\right)} \tag{5}$$

where r_Z is the Z-average solvodynamic radius, PdI is the polydispersity index, and $\gamma(x)$ is the Gamma function $\gamma(x) = \int_0^\infty e^{-t} \cdot t^{x-1} dt$. The corresponding autocorrelation function is

$$g_1(t) = \left(\frac{6 r_Z}{6 r_Z + \mathrm{PdI} \cdot \kappa \cdot Q^2 \cdot t} \right)^{\frac{1}{\mathrm{PdI}}} \tag{6}$$

where $\kappa = \frac{k_B T}{\pi \eta}$. The Z-average and PdI have a central place in DLS analyses, as upon modest polydispeisty, their value approximate the mean and the relative variance (Var/Mean) of the number-based distribution of the solvodynamic radius.

The slow relaxation we describe via a stretched-exponential function, also knowns as Kohlrausch function[20]

$$g_{NF}(t) = e^{-t^\nu / \tau} \tag{7}$$

In this case, we are not at all interested in inferring the values of the two empirical parameters (τ and ν), as we use Equation **7** for a purely phenomenological purpose, we simply need to describe adequately the number fluctuations part in the experimental data relevant tour analysis. Regression was nonlinear and unweighted, minimizing least squares.

The result of the fit is shown in **Figure 2B**. The black line is the coherent scattering of the clusters, while the red dotted line represents the slow relaxation from the number fluctuation. The same fitting routine has been applied to the entire series of clusters, where we noticed significant number fluctuations for the shorter ligands and less so for the longer ligands (**Figure S5-S12**). **Figure 3** shows the average of the size distribution, provide by the above described method and the automatic fit within the Malvern software. The latter also provide the Z-average from the cumulant fit. The high portion of number fluctuations in the samples with short ligands, lead to higher Z-averages and incorrect size distributions. The manual fit more accurately displays the trend of increasing solvodynamic radius of **Zr12** clusters with increasing ligand length. Interestingly, the solvodynamic radius saturates when the ligand reaches a length of 10 carbons. This could be due to ligand configuration changes such as coiling, thus reducing the ligand shell thickness. As a second hypothesis, one can consider a monomer-dimer equilibrium that is affected by the ligand length and which shifts towards monomer for longer chains. Indeed, even in solid state, we have recently shown that the Pair Distribution Function of oleate capped Zr6 clusters, can be described by a mixture of monomer and dimer.[21]

Focusing on the **Zr6** clusters with methylbutanoate and methylheptanoate ligands, we find a similar pattern with a higher portion of number fluctuations for the shorter chain, thus skewing the automatic fitting. However, the manual fit provides reasonable solvodynamic sizes and interesting allows to differentiate monomers from dimers. Indeed, **Zr12**-butanoate clusters appear to have a higher solvodynamic diameter than the **Zr6**-methylbutanoate clusters, despite having the same ligand shell thickness. Interestingly, the solvodynamic diameter did not increase for the clusters with methylheptanoate ligands. Here we cannot invoke a

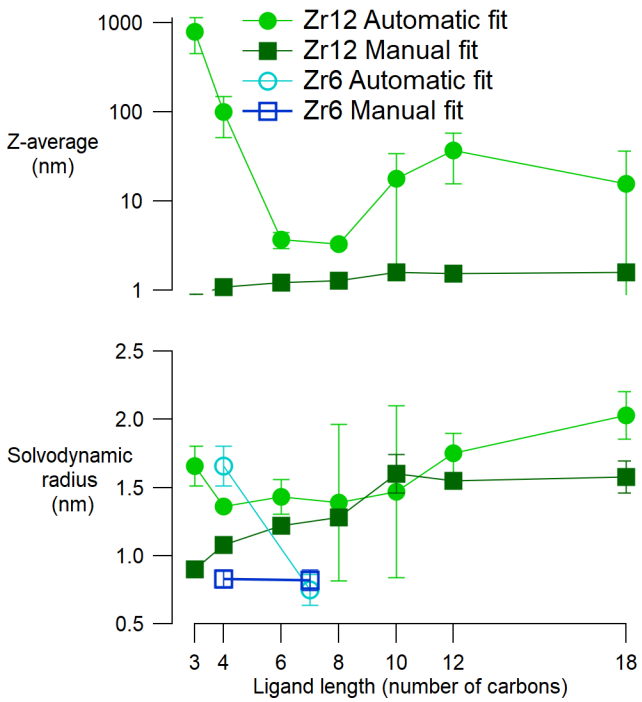

Figure 3: The solvodynamic diameter of the **Zr12** clusters with different ligands (presented by their carbon content), determined either by the automatic fit of the Malvern software and our described fitting routine taking into account the number fluctuation. The average of the size distribution and the Z-average from the cumulant fit are both plotted. The errors are determined based on the triplicate measurements.

monomer-dimer equilibrium to explain the trend and we thus favor the coiling hypothesis.

The effect of the clusters on the viscosity of solvents

Another technique that allows us to study materials in solution is Diffusion Ordered Spectroscopy (DOSY) from which the diffusion coefficient of the species is obtained. Here we subjected both a **Zr12**-butanoate cluster and a **Zr6**-methylbutanoate cluster to a DOSY measurement. Since their ligands have nearly the same length the effect of the ligand on the diffusion coefficient is canceled out and we look merely to the difference between monomeric versus dimeric clusters.

As can be seen from the 2D DOSY plots above both the monomeric (left) and dimeric (right) species diffuse slower compared to the solvent, which is indicated with $CDCl_3$. By fitting the decay, we get precise values for the diffusion coefficients. The diffusion coefficient

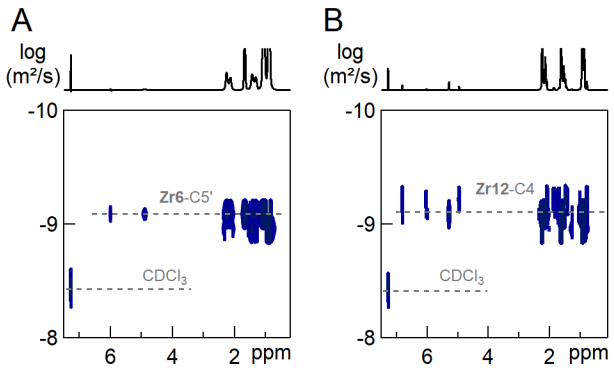

Figure 4: 2D DOSY spectra of both the monomeric (A) and dimeric (B) clusters in a 20 mg/mL concentration in chloroform.

for the monomeric species is 638.28 $\mu m^2/s$ while the dimeric species diffuses slower at a rate of 565.29 $\mu m^2/s$. From these values the diameter of the species can be estimated, by assuming that they are spherical. The monomeric species is estimated to be 1.27 nm whereas the dimeric species is estimated to be 1.43 nm.

By reducing the concentration from approximately 20 mg/mL to only 1 mg/mL we see a big difference indicating that the viscosity of these 20 mg/mL solutions is significantly different from pure chloroform. At 1 mg/mL, the diffusion coefficient for **Zr12**-butanoate is 669.9 $\mu m^2/s$ and the corresponding calculated diameter is therefore only 1.206 nm, which is smaller than previously obtained values. (See SI)

Experimental

The zirconium oxo clusters were synthesized and purified according to our previously published method.[7] All measurements were performed with a Zetasizer Ultra instrument (Malvern Panalitical) equipped with a HeNe laser (633 nm, 10 mW) and an APD detector. The respective amount of cluster was weighed into a 4 mL-vial, and solvent was added until the required concentration was reached. Next, the solution was filtered (Acrodisc one, GFX/0.2 µm wwPTFE) into a glass cuvette with square aperture (PCS1115) to remove dust from the solution. The following material settings were used: for ZrO_2, refractive in-

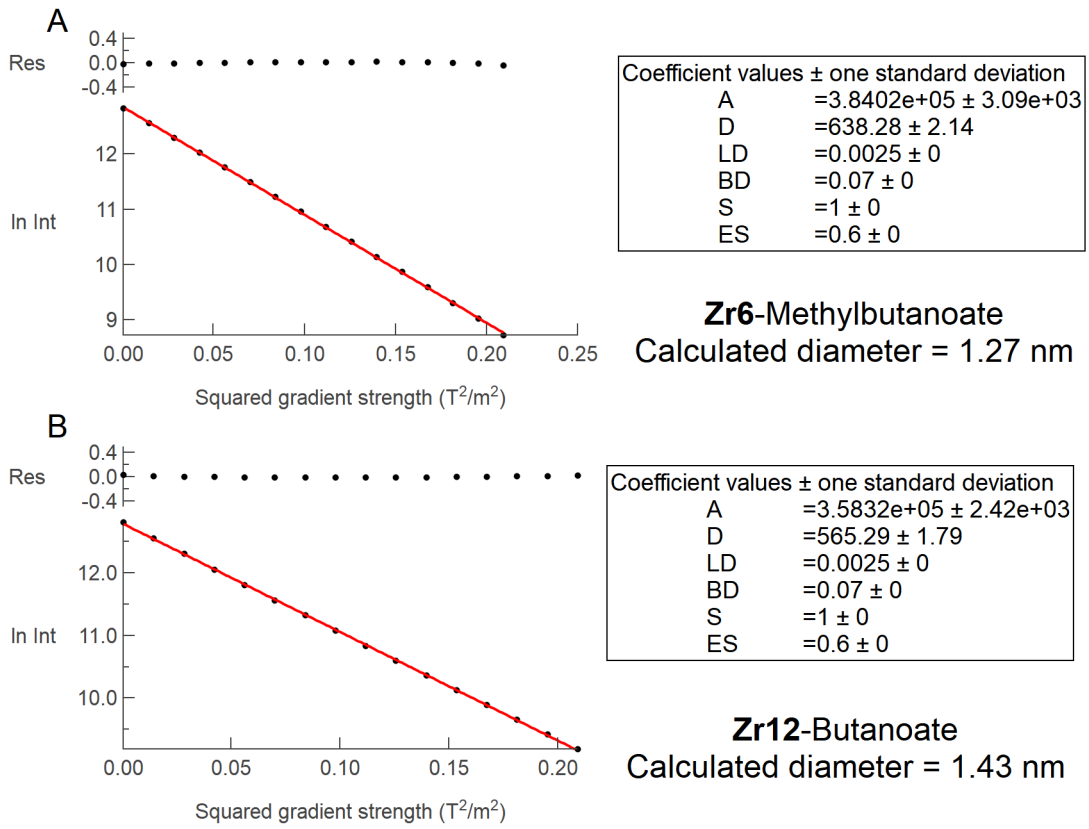

Figure 5: Fit of the DOSY data for both the monomeric (A) and dimeric (B) cluster species with a concentration of 20 mg/mL in chloroform. Based on the fit the diffusion coefficient is obtained which is subsequently used to estimate the solvodynamic radius.

dex = 2.15 and absorption = 0.001; for the solvent (chloroform) refractive index = 1.45 and viscosity = 0.563 mPa.s. Before each measurement, the instrument was equilibrated at 25°Cfor 120 s, and each measurement was run 3 times. DLS spectra were collected in batch mode, measuring unfractionated samples, using adaptive correlation, which benefits from the statistical analysis of short runs, and aims to produce the most sample-representative and 'steady-state' correlation function.

DOSY measurement

For the DOSY measurement 0.0058 mmol cluster (10 mg **Zr12**-C4, 10.94 mg **Zr6**-C5') was dissolved in 500 µL $CDCl_3$. Of this solution 100 µL was added to a 3 mm NMR tube which was fitted inside a 5 mm NMR tube. P1 was determined to 10.663 ms for **Zr12**-C4 and

10.675 ms for **Zr6**-C5'. D20 and p30 were equal for both measurements and were 0.07 and 1250, respectively.

Acknowledgement

The authors thank the SNF NCCR molecular systems engineering (182895) and the Swiss Nanoscience Insitute for funding.

Supporting Information Available

DLS fittings with script, viscosity calculations.

References

(1) Bezrukov, A. A.; Törnroos, K. W.; Le Roux, E.; Dietzel, P. D. C. Incorporation of an intact dimeric Zr12 oxo cluster from a molecular precursor in a new zirconium metal–organic framework. *Chemical Communications* **2018**, *54*, 2735–2738.

(2) Huang, J.-Y.; Xu, H.; Peretz, E.; Wu, D.-Y.; Ober, C. K.; Hanrath, T. Three-Dimensional Printing of Hierarchical Porous Architectures. *Chemistry of Materials* **2019**, *31*, 10017–10022.

(3) Moons, J.; de Azambuja, F.; Mihailovic, J.; Kozma, K.; Smiljanic, K.; Amiri, M.; Cirkovic Velickovic, T.; Nyman, M.; Parac-Vogt, T. N. Discrete Hf18 Metal-oxo Cluster as a Heterogeneous Nanozyme for Site-Specific Proteolysis. *Angewandte Chemie International Edition* **2020**, *59*, 9094–9101.

(4) Van den Eynden, D.; Pokratath, R.; De Roo, J. Nonaqueous Chemistry of Group 4 Oxo Clusters and Colloidal Metal Oxide Nanocrystals. *Chemical Reviews* **2022**, *122*, 10538–10572, PMID: 35467844.

(5) Kickelbick, G.; Schubert, U. Oxozirconium Methacrylate Clusters: Zr6(OH)4O4(OMc)12 and Zr4O2(OMc)12 (OMc = Methacrylate). *Chemische Berichte* **1997**, *130*, 473–478.

(6) Puchberger, M.; Kogler, F. R.; Jupa, M.; Gross, S.; Fric, H.; Kickelbick, G.; Schubert, U. Can the Clusters Zr6O4(OH)4(OOCR)12 and [Zr6O4(OH)4(OOCR)12]2 Be Converted into Each Other? *European Journal of Inorganic Chemistry* **2006**, *2006*, 3283–3293.

(7) Van den Eynden, D.; Pokratath, R.; Mathew, J. P.; Goossens, E.; De Buysser, K.; De Roo, J. Fatty acid capped, metal oxo clusters as the smallest conceivable nanocrystal prototypes. *Chem. Sci.* **2023**, *14*, 573–585.

(8) Cummins, H. Z.; Pusey, P. N. *Photon Correlation Spectroscopy and Velocimetry*; Springer US: Boston, MA, 1977; pp 164–199.

(9) Schaefer, D. W.; Berne, B. J. Light Scattering from Non-Gaussian Concentration Fluctuations. *Physical Review Letters* **1972**, *28*, 475–478.

(10) Nijman, E.; Merkus, H. G.; Marijnissen, J. C. M.; Scarlett, B. Simulations and experiments on number fluctuations in photon-correlation spectroscopy at low particle concentrations. *Applied optics* **2001**, *40*, 4058–4063.

(11) Ferreira, D.; Bachelard, R.; Guerin, W.; Kaiser, R.; Fouché, M. Connecting field and intensity correlations: The Siegert relation and how to test it. *American Journal of Physics* **2020**, *88*, 831–837.

(12) Einstein, A. The motion of elements suspended in static liquids as claimed in the molecular kinetic theory of heat. *Ann Phys-Berlin* **1905**, *17*, 549–560.

(13) Einstein, A. Eine neue Bestimmung der Moleküldimensionen. *Annalen der Physik* **1906**, *324*, 289–306.

(14) Einstein, A. Berichtigung zu meiner Arbeit: Eine neue Bestimmung der Moleküldimensionen. *Annalen der Physik* **1911**, *339*, 591–592.

(15) Debye, P. *Polar molecules*; Dover: New York, 1929.

(16) Peebles, P. Z. *Probability, Random Variables and Random Signal Principles*; New York : McGraw-Hill, 1987.

(17) Schulz, G. The kinetics of chain polymerisation V. The influence of various types of reactions on the poly-molecularity. *Z Phys Chem B-Chem E* **1939**, *43*, 25–46.

(18) Zimm, B. H. Apparatus and Methods for Measurement and Interpretation of the Angular Variation of Light Scattering; Preliminary Results on Polystyrene Solutions. *The Journal of Chemical Physics* **1948**, *16*, 1099–1116.

(19) Balog, S.; Rodriguez-Lorenzo, L.; Monnier, C. A.; Michen, B.; Obiols-Rabasa, M.; Casal-Dujat, L.; Rothen-Rutishauser, B.; Petri-Fink, A.; Schurtenberger, P. Dynamic Depolarized Light Scattering of Small Round Plasmonic Nanoparticles: When Imperfection is Only Perfect. *The Journal of Physical Chemistry C* **2014**, *118*, 17968–17974.

(20) Kohlrausch, R. Theorie des elektrischen Rückstandes in der Leidener Flasche. *Annalen der Physik* **1854**, *167*, 179–214.

(21) Pulparayil Mathew, J.; Seno, C.; Jaiswal, M.; Simms, C.; Reichholf, N.; Van den Eynden, D.; Parac-Vogt, T. N.; De Roo, J. The Central Role of Oxo Clusters in Zirconium- and Hafnium-Based Esterification Catalysis. *ChemRxiv* **2024**,

TOC Graphic